

Evaluation of Rutting Behaviour of Geocell Reinforced Sand Subgrades Under Repeated Loading

Sireesh Saride · Vijay K. Rayabharapu ·
Suraj Vedpathak

Received: 28 December 2013 / Accepted: 8 May 2014 / Published online: 22 May 2014
© Indian Geotechnical Society 2014

Abstract This paper summarizes the results from a series of large scale cyclic model load tests on geocell reinforced and unreinforced homogeneous sand subgrades. The sand subgrades are prepared at 70 % relative density thru pluviation technic in a large steel tank measuring 1 m³. A cyclic load of 0.7 and 7 kN was applied on a circular steel plate of 150 mm diameter to replicate a portion of load transfer from an equivalent single axle wheel load (ESAL) on the sand subgrade. The cyclic load was applied through a double acting dynamic hydraulic 100 kN actuator. A series of tests were conducted to study the effects of width and height of a geocell reinforcement on the cyclic behavior of sand subgrades. The performance improvement is quantified in terms of traffic benefit ratios (TBR), cumulative plastic deformations (CPD), modulus of subgrade reaction (k_s), resilient modulus (M_r) and rut depth reduction (RDR) for different number of cycles and plate settlements. The configuration of the geocell that provides highest performance in terms of TBR, CPD, and RDR, is considered to be the optimum size of the geocell. It is observed that the optimum geometry of the geocell is capable of reducing the rut depth of about 75 % at 100 cycles and provide about a TBR of 23 at 10 % of settlement ratio.

Keywords Geocell reinforcement · Traffic load · Traffic benefit ratio · Plastic deformations · Rut depth

List of symbols

b	Width of geocell
D	Diameter of the loading plate
h	Height of geocell
N	Number of loading cycles
n	n th number of loading cycle
u	Depth of placement of reinforcement from the surface
s	Plate settlement
CPD	Cumulative permanent deformation, %
RDR	Rut depth reduction, %
TBR	Traffic benefit ratio

Introduction

The major concern of any flexible pavement or low volume road is the phenomenon of *rutting*. Usually low volume roads are paved with asphalt concrete or unpaved in nature. Rutting can be described as a depression or settlement on a road surface due to traffic loading or compression or settlement of any pavement layers or weak subgrade. Excessive rutting can be avoided by using good quality construction materials in pavement layers or stabilization of subgrade soils or combination of both. The rutting behavior of weak subgrade soils can be improved by inserting a planar geosynthetic layer at the interface of subgrade soil and the base/subbase layer. A large variety of geosynthetic products manufactured of different polymers are being used in various geotechnical and transportation

S. Saride (✉) · V. K. Rayabharapu · S. Vedpathak
Department of Civil Engineering, Indian Institute of Technology
Hyderabad, Ordnance Factory Campus,
Yeddemailaram 502 205, Andhra Pradesh, India
e-mail: sireesh@iith.ac.in

V. K. Rayabharapu
e-mail: vkraya@gmail.com

S. Vedpathak
e-mail: vedpathaksd@gmail.com

applications. Recently, a three dimensional form of geosynthetics, called geocells, which provide higher load carrying capacity have been in use in pavement layers.

Studies on geocell reinforcement for pavement applications were started about half a century ago for the first time by US Army Corps of Engineers for improving the bearing capacity of poorly graded sand by using it as a lateral confinement [1]. The important reinforcement mechanisms for geocell reinforcement are lateral confinement, increased bearing capacity, and tensioned membrane effects [2–4]. Bending resistance, tensile strength, and shear strength, and intercept of the failure planes from the subgrade are observed when geocells were used in pavement bases [5]. These mechanisms are mostly instigated from static plate load tests, however in reality; the traffic loading is cyclic in nature. Very limited literature is available to date to understand the cyclic/dynamic behavior of geocell reinforced subgrades. Hence, in this paper, results from a series of cyclic load tests on geocell reinforced sand subgrades are presented.

Background

Different reinforcement forms are being used for a long time viz. geotextiles, geogrids, geonets, geocomposites and geocells. Extensive literature is available on these materials as reinforcement (geogrids and geocells) under static loading for pavement applications [3, 6–10], however, a very few studies are available on cyclic loading. Base course lateral restraint is the main reinforcement mechanism of geosynthetics in paved roads as described by Bender and Barenberg [11]. Further, Kinney and Barenberg [12] demonstrated that the geotextile-reinforcement can be used in unpaved roads. Hossein et al. [13] reported that under cyclic loadings, the settlement over the loading area of reinforced pavement is reduced when compared with unreinforced pavement.

The benefits with geosynthetic reinforcements in pavements under cyclic loading are computed as a non-dimensional term called traffic benefit ratio (TBR). TBR can be expressed in terms of extension of life or by savings in base course thickness. TBR is defined as the ratio of the number of cycles necessary to reach a given rut depth for a section containing reinforcement, divided by the number of cycles necessary to reach the same rut depth for an unreinforced section with the same section thickness and subgrade properties. This parameter is consistent with the non-dimensional parameter called improvement factor defined in the case of static loading system on geosynthetic reinforced foundation beds [3, 9, 10].

Studies investigated on cyclic behavior of different forms of geosynthetic reinforcements provided the TBRs.

Barker [14] observed a TBR of 1.2 with geogrid reinforcement under a moving single wheel system in an outdoor test track applying 120 kN load. Haas [15] reported that a TBR of about 3.3 was obtained for geogrid reinforced beds in a large laboratory test tank of dimensions 4.5 m × 1.8 m × 0.9 m using a stationary circular plate of 300 mm diameter corresponding to the pressure of 550 kPa at a frequency of 8 Hz. Barksdale [6] and Collin [8] have observed a TBR of 2.8 and 2.3 when applied a moving single wheel applying a pressure of 500 kPa on indoor test track respectively. Combination of geogrid and geotextile reinforcements in a large test tank of size 3.1 × 1.8 × 2.1 resulted in a TBR range of 1.7–3.0 under a standard axle load of 550 kPa applied through a 300 mm diameter plate by Al-Qadi et al. [16] and Cancelli et al. [7]. Large-scale cyclic loading tests on geocells were studied by Pokharel [17] and observed that the geocells have improved the strength, increased the percentage of elastic deformation and life of the unpaved road sections over weak subgrade. Saride et al. [18] observed that the permanent deformations were reduced by 8 fold and TRBs were increased to 45 for the case of geocell size $h/D = 1$, $b/D = 4$ against the unreinforced bed at 5 % plate settlement under traffic load of 400 kPa.

Kazerani and Jamnejad [19] observed that the strength of the subgrade and the quality of infill material play a vital role in improving the performance of the geocell-reinforced road sections subjected to cyclic loading. Higher performance was observed with geocell reinforcement with dense infill on a good subgrade. Similar observations were reported by Han et al. [4] that the placement of geocell from the surface of loading is also crucial. In contrary, the placement depth of geocell should be maintained at about 1–5 % of the width of the loading area in static load tests as observed in Dash et al. [3] and Sitharam and Sireesh [10].

Literature study reveals based on the limited information available on geocells, that the behavior of geocell reinforced beds under repeated loading is not yet understood completely in terms of rutting. Hence, in this study, an attempt has been made to understand the rutting behavior of geocell reinforced sand subgrades under repeated traffic loading.

Materials and Methods

Sand

The soil used in this investigation was dry sand. The particle size distribution of the sand was determined by dry sieve analysis [20]. The particle size distribution of the sand is shown in Fig. 1. The sand is classified as poorly graded sand with letter symbol SP according to the unified soil classification system (USCS).

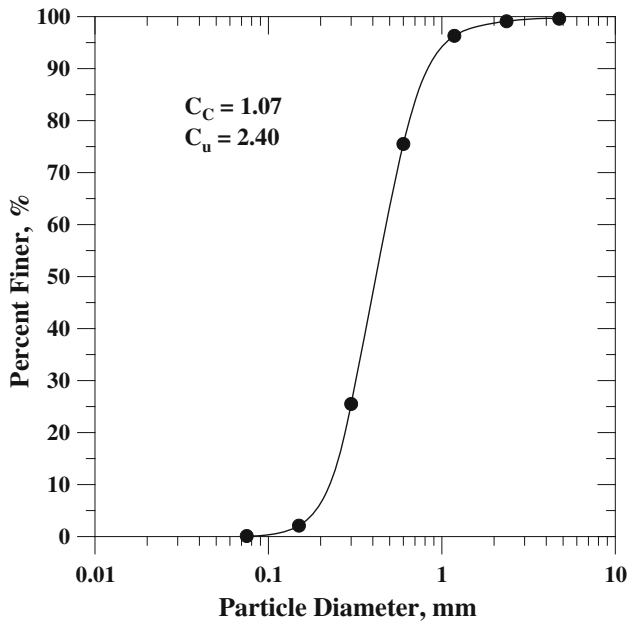


Fig. 1 Particle size distribution curve for sand

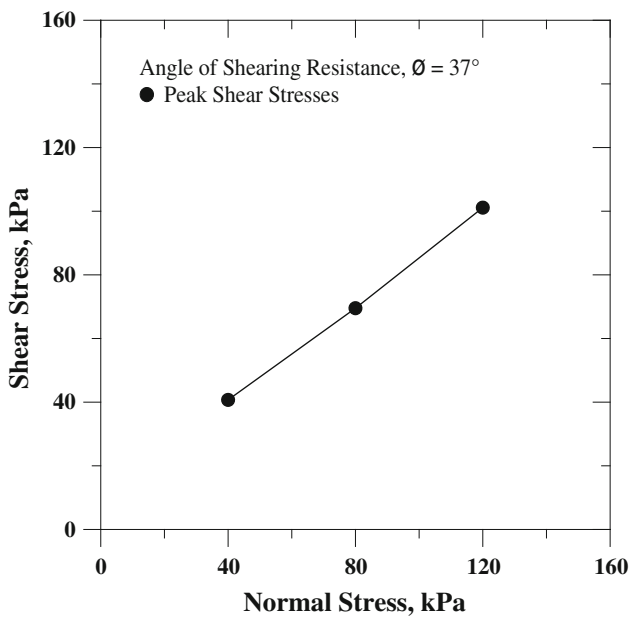


Fig. 2 Variation of shear stress with normal stress

The physical properties such as specific gravity, maximum and minimum void ratios of sand were determined [21–23] respectively. Direct shear tests [24] were conducted on unreinforced sand in a small shear box of dimensions 100 mm × 100 mm × 30 mm. The sand was compacted at its 70 % relative density and subjected to normal pressures corresponds to 40, 80 and 120 kPa to obtain the angle of shearing resistance of sand as shown in Fig. 2. All the properties of sand are presented in Table 1.

Table 1 Properties of sand used in the study

Properties	Values
D_{10} , mm	0.20
D_{30} , mm	0.32
D_{60} , mm	0.48
C_u	2.40
C_c	1.07
Specific gravity, G_s	2.63
e_{max}	0.74
e_{min}	0.51
$\phi @ R_D = 70 \%$	37°



Fig. 3 Typical geocell mattress used in the study

Geocell

Geocell is a strong, lightweight, three dimensional cellular confinement system, which is made of ultrasonically-welded high density polyethylene (HDPE) strips that are expandable on-site to form a honeycomb-like structure. A typical geocell mattress used in the study can be seen in Fig. 3.

The geocell used in the present study is manufactured from a polymer of HDPE material with a density ranging between 0.935 and 0.965 g/cm³ having a weld at regular intervals of 400 mm. The properties of the geocells are presented in Table 2.

Test Setup

Uniform sand beds with 70 % relative density were prepared in a test tank measuring inner dimensions of

Table 2 Properties of Geocell

Properties	Values
Material composition	Polymer—high density polyethylene (HDPE)
Density, g/cm ³	0.935–0.965
Weld spacing (mm)	400
Cell depth (mm)	75, 100, 150
Min. cell seam strength (N)	1,050, 1,400, 2,100

1 m × 1 m × 1 m (length × width × height). A rigid steel plate of 150 mm diameter (D) and 15 mm thickness was used to apply the repeated traffic loading on the sand subgrades. The diameter of the loading plate and the dimensions of the tank were decided based on the literature. Chummar et al. [25] observed the failure wedge, below footing plate, on a sand bed is extended around 2–2.5B on either side of the footing and to a depth of around 1.1D from the bottom of the footing, where D is the diameter of the footing. In addition, to check the boundary effects on the experimental results from reinforced test beds, strain type earth pressure transducers were placed at the boundaries of the tank and the pressures were measured using a data acquisition system. Minimal pressures (less than 1 % of the applied pressure) have been recorded affirming that the influence of the boundary on the test results is negligible. Similar kind of plate diameter and test tank were adopted by Edil et al. [26] in their laboratory experiments on geosynthetic reinforced pavements. The schematic of the test bed used in the present study can be seen in Fig. 4. Loading was given by graphical user interfaced multi-purpose test software along with the help of hydraulic power unit, hydraulic service manifold and sophisticated double acting linear dynamic 100 kN capacity actuator which is attached to a 3.5 m high, 200 kN capacity reaction frame as shown in Fig. 5.

Testing Procedure

Test procedure involves the development of calibration graph for sand pluviation, sand bed preparation with and without geocell reinforcement and repeated load tests.

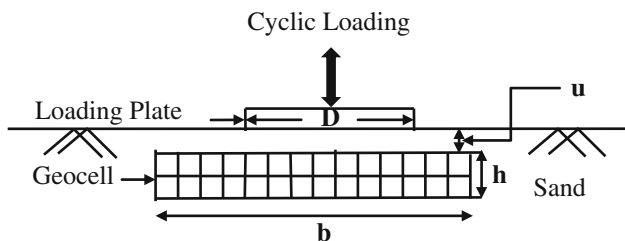


Fig. 4 Schematic of test setup

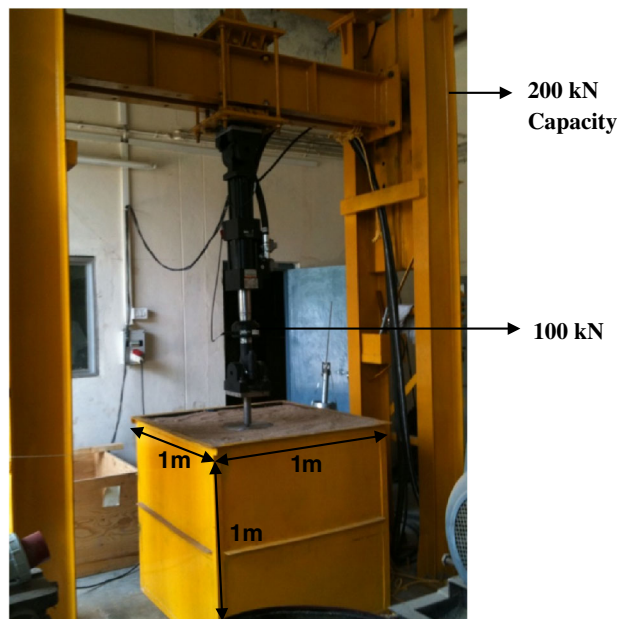


Fig. 5 Test-cum-loading system used in the study

Relative Density Calibration Chart

A uniform relative density of the sand was maintained in the test tank using a known technic called sand raining or sand pluviation. To achieve a uniform density, a pluviation device (pluviator) is designed for this purpose. A 40 mm internal diameter and 300 mm long stand pipe with an inverted cone welded at its one end was attached to the bottom of the hopper. The sand from the hopper is poured through the pluviator which is dispersed at bottom by a 60° inverted cone. The pluviator is attached with a movable scale to maintain different heights of fall of sand.

To maintain a desired relative density (R_D) of sand in the test tank, sand has to be pluviated from certain height. The height of fall decides the relative density of the sand that can be maintained. Natural densities were measured physically by collecting samples in small containers whose weights and volumes were known from each case. With the known values of the minimum and maximum void ratios of sand, a calibration chart was prepared for the height of fall against the corresponding relative density of the sand. For any required relative density, the corresponding height of fall can be read directly from the calibration chart.

Sand Bed Preparation

The test tank was filled with the sand using pluviation technique as discussed earlier. The relative density of sand in this study was maintained at 70 %. The density of test bed was frequently monitored by taking samples at

different depths during pluviation. The densities were well within the range of 2 % error.

After filling the test tank with the sand up to the desired height, the fill surface was leveled and the loading plate was placed on a predetermined alignment such that the loads from the actuator applied would be transferred concentrically to the footing. To facilitate this, a recess was made into the loading plate at its center to accommodate a ball bearing through which vertical loads were applied to the plate. In the case of reinforced beds, upon ceasing the pluviation at predetermined depth, the geocell was positioned and stretched on the leveled subgrade and continued the sand pluviation to fill the geocell mattress with the same density.

Repeated Load Tests

A portion of repeated Equivalent single axle wheel load was applied on to the loading plate using a computer-controlled servo hydraulic actuator, with a maximum load of 7 kN and a minimum of 0.7 kN (10 % of the maximum load) using a continuous haversine loading pattern as shown in Fig. 6 at a frequency of 0.77 Hz as described in Saride et al. [18]. The loading pattern was chosen such a way that it replicates the moving traffic on the pavement. The maximum pressure (corresponds to about 400 kPa) on the subgrade was also confirmed by conducting static load tests on unreinforced beds which would not exceed the ultimate bearing pressure, which is about 440 kPa, on the sand subgrades. In addition, Saride et al. [27] have measured similar pressures on the subgrades from field trials using a strain type total earth pressure cells buried under GSB layer just above the subgrade. Since the intermediate pavement layers have not been simulated in this model tests, the pressure exerted on to the subgrade was directly applied through a plate. Multi-purpose test ware software was set up to control and acquire the applied load data as well as the deformation data.

A series of repeated load model tests were conducted to verify the efficiency of the geocell layers in the subgrade to mitigate the subgrade rutting as presented in Table 3. The width and height of geocell mattresses are expressed in terms of normalized ratios with respect to diameter of the loading plate as b/D and h/D respectively. The model tests include unreinforced tests, single geocell layers with different sizes (width and height) with respect to the plate diameter. Series A includes unreinforced subgrade tests. The effect of width of geocell at $b/D = 2.33, 3.5$ and 4.33 on the rutting behavior of subgrade is verified in Series B. The third series includes the variation of height of the geocell at $h/D = 0.5, 0.67$ and 1.0 . In geocell reinforcement, seam strength plays an important role in load carrying capacity, as the seam is the weakest zone in geocell

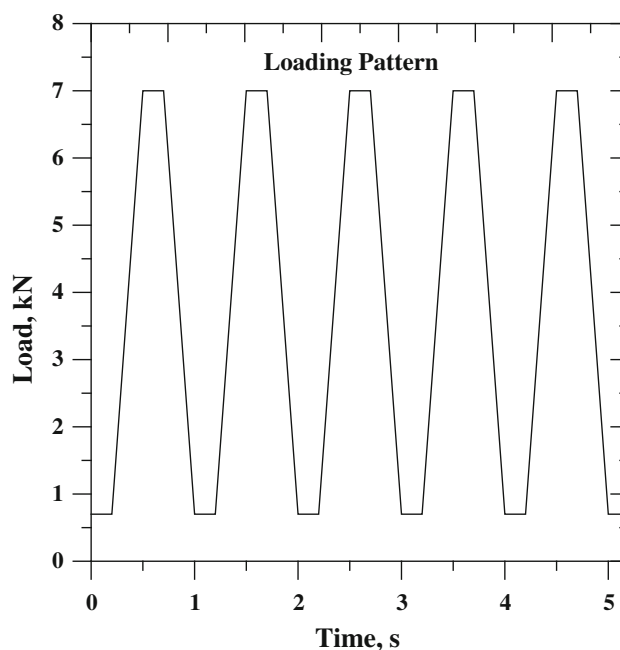


Fig. 6 Loading pattern used in the study

mattress. Test series-D includes tests on load application directly on weld and a cell pocket of the geocell mattress for an $h/D = 1.0$ and $b/D = 1.5$. This series is to quantify the efficacy of the weld under a repeated traffic loading. The depth of the reinforcement layer from the bottom of the plate was maintained at 0.1 times the diameter of the plate (u/D) according to Sitharam and Sireesh [10] and Dash et al. [3]. The equivalent diameter of geocell pockets, d_c was maintained at about $1.6D$ in all the tests. Tests were terminated while reaching a plate settlement of about 25 %.

Results and Discussion

General

Results from different repeated plate load tests are obtained in terms of pressure-settlement responses. A typical response of geocell reinforced sand subgrade under repeated loading in terms of pressure settlement and time settlement are shown in Figs. 7 and 8 for a geocell configuration of $h/D = 1, b/D = 4.33$. The total settlement ratio, s/D , defined as the ratio of plate settlement and the diameter of the plate, is higher for the initial loading cycles, while their magnitude attenuates with number of cycles. To analyze the data in terms of permanent deformations (rutting), the total settlement accumulated from each cycle has been split into two components viz. elastic and plastic settlements as shown in Fig. 9. The plastic

Table 3 Test series done in this study

Test series	Description	Constant parameters	Variable parameters
A	Unreinforced bed	$R_D = 70 \%$	None
B	Geocell reinforced bed	$R_D = 70 \%$, $h/D = 0.67$, $u/D = 0.1$	$b/D = 2.33, 3.5, 4.33$
C	Geocell reinforced bed	$R_D = 70 \%$, $b/D = 4.33$, $u/D = 0.1$	$h/D = 0.5, 0.67, 1.0$
D	Geocell reinforced bed	$R_D = 70 \%$, $b/D = 2.33$, $h/D = 1.0$, $u/D = 0.1$	Load on weld, load on cell

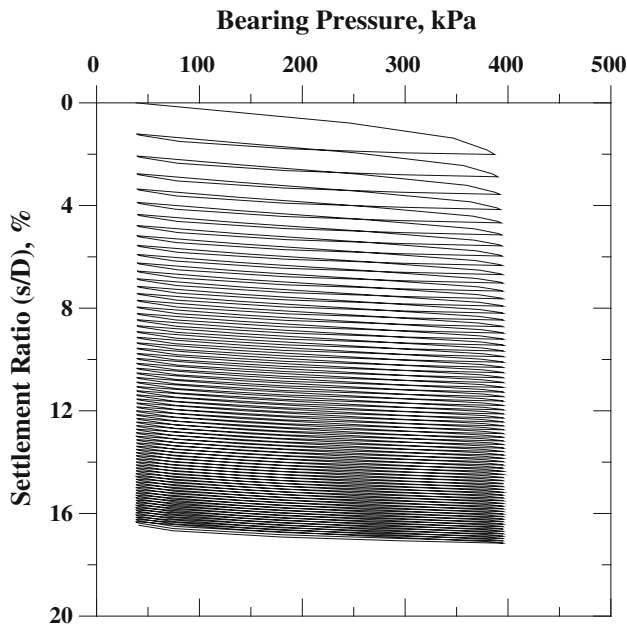


Fig. 7 Typical cyclic pressure-settlement curve

settlements (permanent deformations) are cumulatively added to obtain cumulative permanent deformations (CPDs) expressed in percentage of plate diameter. Further, the data is also presented in terms of TBRs as defined in background section earlier.

To quantify the rutting behavior of geocell reinforcement, a parameter rut depth reduction (RDR), expressed in percentage, for different cases studied as per Table 3 is introduced. RDR can be defined as the ratio of difference between cumulative permanent deformations of the unreinforced bed and geocell reinforced bed to that of the unreinforced bed for a particular number of loading cycle. Hence, RDR for an n th load cycle can be expressed as:

$$(RDR)_{N=n} = \left(1 - \frac{CPD_{rein}}{CPD_{unrein}} \right)_{N=n} \times 100$$

Similar performance parameter, percentage reduction in footing settlement (PRFS) was introduced by Moghaddas et al. [28] to quantify the performance of footing resting on geocell reinforced beds under cyclic loading. Results from test series-A show that the unreinforced test beds could not sustain any number of loading cycles before they reach the

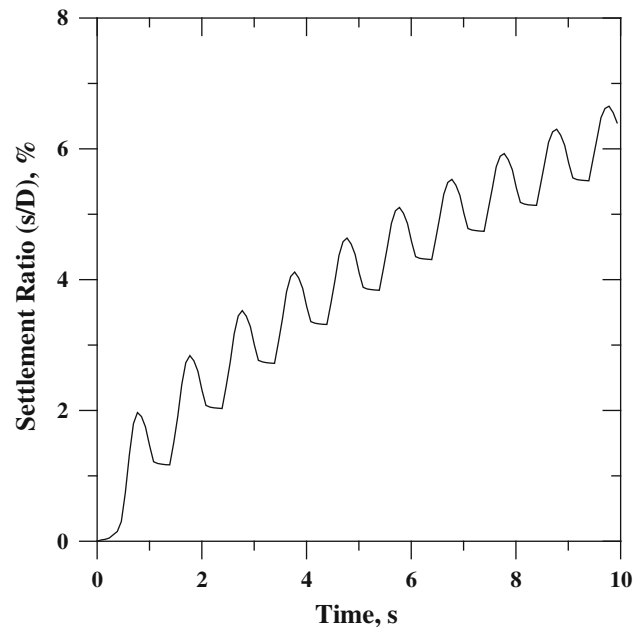


Fig. 8 Typical time-settlement curve

prescribed plate settlement of 25 %. Hence, the settlement ratios were allowed to exceed more than 50 %, though there is no practical significance of this range of settlements, to quantify number of cycles to determine the TBRs. The data from test series-A shows that the unreinforced subgrade reached maximum amount of settlement in only few loading cycles. It can be seen that the cumulative permanent deformations are as high as 75 % in unreinforced bed.

To further quantify the performance of the beds under repeated loading, mechanistic parameters like modulus of subgrade reaction (k_s) and resilient modulus (M_r) are presented. These parameters are calculated based on the stress applied and the elastic response of the subgrade. k_s is computed as the ratio of the applied stress and the elastic deformation and M_r as the ratio of applied stress and elastic strains from the response of the subgrade. The elastic settlements were considered corresponding to those cycles where the settlements become asymptotic to x axis (steady state strain). The unreinforced subgrade is having a k_s and M_r of about 474 MN/m^3 and 62 MPa respectively. The

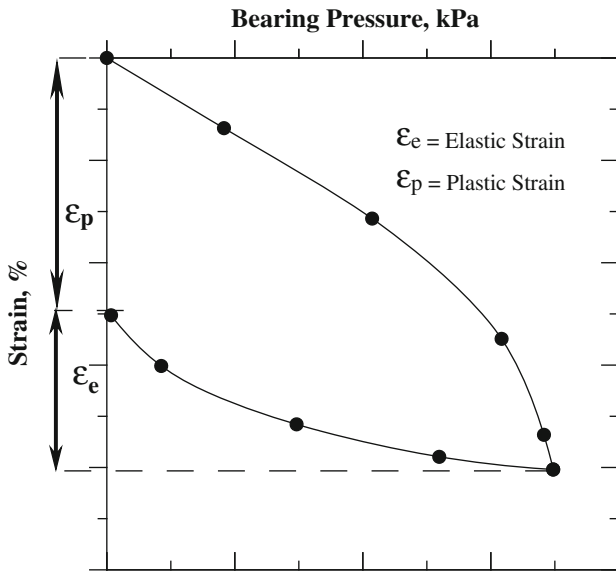


Fig. 9 Elastic and plastic strains of a typical loading cycle

results from test series B, C and D are presented in Table 4 and discussed in the following sections.

Effect of Geocell Width

Results obtained from test series-B, with the variation of $b/D = 2.33, 3.5$ and 4.33 for a constant $h/D = 0.67$, are presented in Figs. 10 and 11 in terms of CPDs and TBRs respectively. The variations of CPDs with number of loading cycles are presented in Fig. 10. Though the number of load cycles sustained by geocell reinforced subgrades are much higher (in thousands) before exhibiting 25 % plate settlement, only 50 load cycles ($N = 50$) are presented to visualize the CPD variations for various geocell width ratios. The CPDs of geocell reinforced beds are much lower than that of unreinforced subgrades. These drastic reductions in permanent deformations are noted as high as 2, 3 and 4 fold for the cases of $b/D = 2.33, 3.5$ and

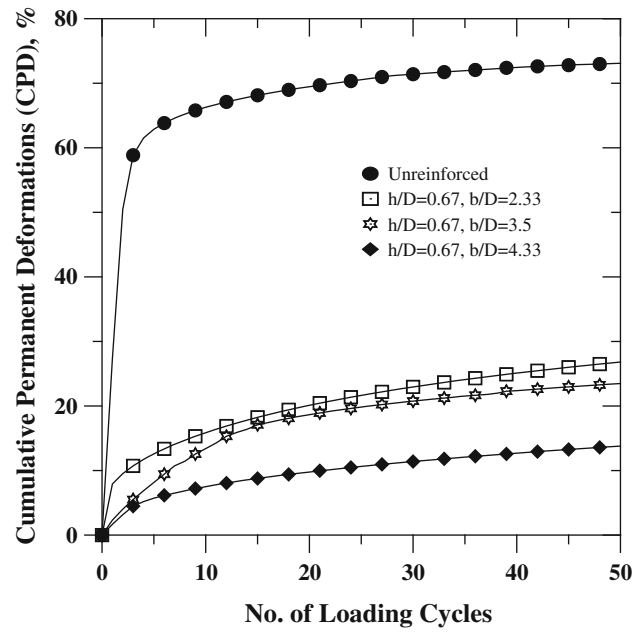


Fig. 10 Variation of CPD with number of cycles—Series B

4.33 respectively against unreinforced bed. The reduction in CPDs for geocell reinforced subgrades against unreinforced subgrades can be attributed to the increase in elastic response of geocell reinforced subgrades. This response has increased with increase in geocell width ratio.

The variation of TBR with settlement ratio, s/D is presented in Fig. 11. The TBR increases with increase in the s/D ratio and width ratio of geocell mattress (b/D). The TBR at $s/D = 10\%$ are observed to be 2, 10 and 18 for $b/D = 2.33, 3.5$ and 4.33 respectively. It can be inferred from this figure that to obtain higher structural support for the pavement layers, the geocell width should be adequate enough to provide resilient response. The values of k_s are 492, 544, 586 MN/m^3 and M_r are 72, 74, 88 MPa for $b/D = 2.33, 3.5$ and 4.33 respectively.

The influence of geocell width on the performance of rutting behavior is presented in Fig. 12. The RDR in

Table 4 Results from test series A–D

Test series	Variable parameters	CPD (%) at $N = 50$	Modulus of subgrade reaction k_s (MN/m^3)	Resilient modulus M_r (MPa)
A	Unreinforced	72	474	62
B	$b/D = 2.33$	27	492	72
	3.5	23	544	74
	4.33	14	586	78
C	$h/D = 0.5$	36	538	74
	0.67	14	586	78
	1.0	13	588	88
D	Load on weld	42	481	63
	Load on cell	53	487	64

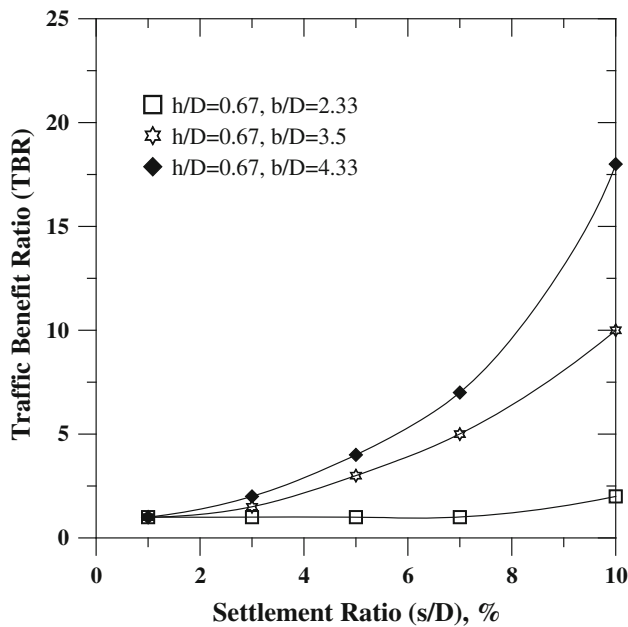


Fig. 11 Variation of TBR with settlement ratio—Series B

percentage is expressed at various number of load cycles ($N = 1, 5, 10, 50$ and 100) with the geocell width ratio, b/D . The percentage reduction in rut depth with number of load cycles has reduced. This is attributed to the reduction in permanent deformations due to densification of subgrade soil and cumulative resilient behavior of geocell reinforcement with increase in number of load cycles. The reduction in rut depth increased with increase in b/D with a maximum value of 75 % for $b/D = 4.33$ at $N = 100$. Based on the above discussion from the present study, the optimum width ratio (b/D) of the geocell mattress may be considered as 4.33. This observation is in confirmation with the results obtained by Dash et al. [3] and Shin et al. [29] on large scale tests on geocell and geogrid reinforced sand beds respectively. More recently, Faby Mole et al. [30] have concluded from their numerical analysis on geocell reinforced subgrades supporting strip footing that there would not be any performance improvement in the system if the geocell reinforcement is extended beyond a width ratio of about 5. This confirms that the optimum size of geocell width would be around 5 times the size of the loading plate.

Effect of Geocell Height

The test series-C includes the variation of height ratio of the geocell mattress, $h/D = 0.5, 0.67$ and 1.0 for a constant $b/D = 4.33$. The variation of cumulative permanent deformations with number of loading cycles is shown in Fig. 13. The variation of TBR with settlement ratio is presented in Fig. 14.

The cumulative permanent deformations of geocell reinforced beds are reduced with increase in the height of the

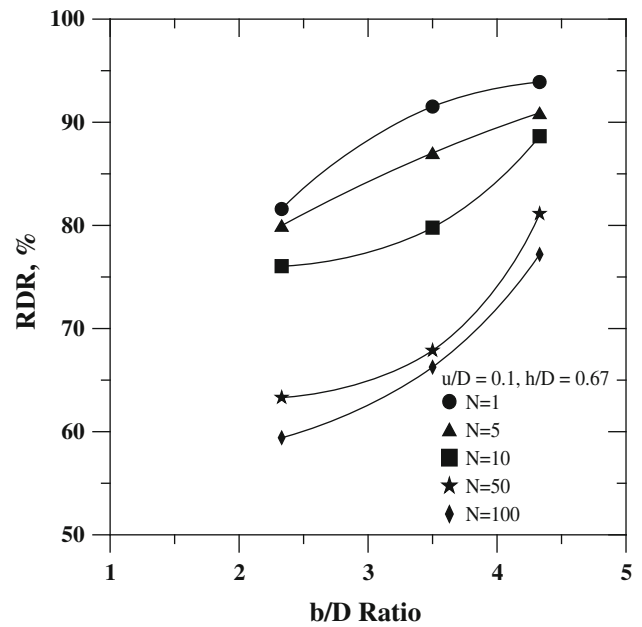


Fig. 12 Variation of RDR with b/D ratio—Series B

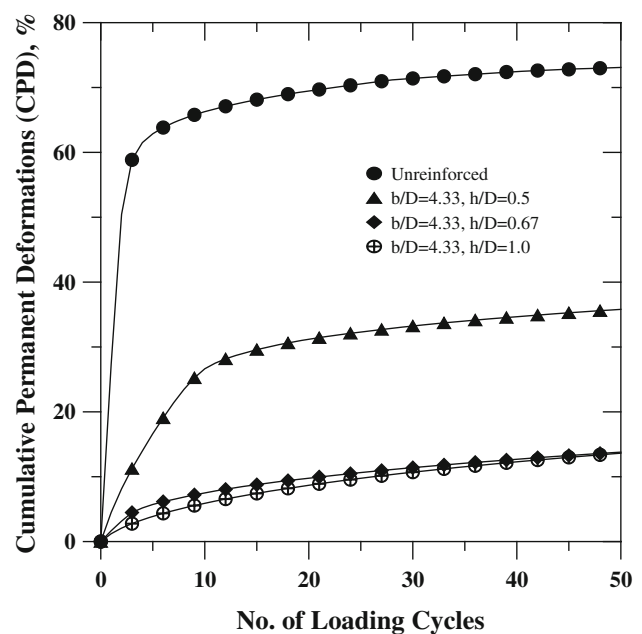


Fig. 13 Variation of CPD with number of cycles—Series C

geocell mattress (Fig. 13). This reduction is observed up to $h/D = 0.67$ from $h/D = 0.5$. Further increase in height of geocell mattress did not show much performance improvement in terms of reduction in the permanent deformations. The reduction in CPDs are observed to be 2, 4 and 5 fold against unreinforced subgrades for $h/D = 0.5, 0.67$ and 1.0 respectively. It is to be noted here that the permanent deformations are higher for the case of $h/D = 0.5$ with $b/D = 4.33$. The higher permanent deformations, in this case, can be attributed to the least flexural stiffness of the

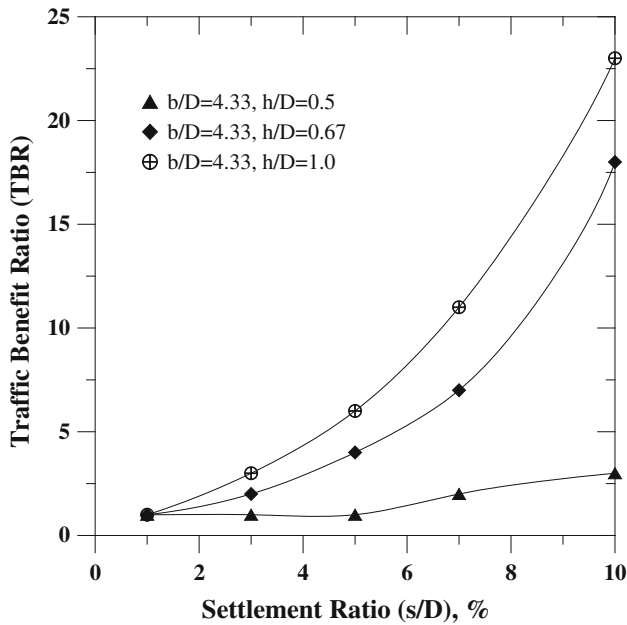


Fig. 14 Variation of TBR with settlement ratio—Series C

geocell mattress available compared to the other two cases. Lower permanent deformations observed in the other cases are due to the provision of enough structural support extended by the geocell mattress of heights, $h/D = 0.67$ and 1.0 by virtue of encapsulating all the potential failure surfaces within the reinforced subgrade zone.

The TBRs at 10 % settlement ratio are observed to be 3, 18 and 23 respectively for $h/D = 0.5, 0.67$ and 1 . It can also be inferred from Fig. 14 that for obtaining higher structural support for the pavement layers, the geocell height should be adequate enough to provide resilient behavior. The modulus of subgrade reaction and resilient modulus values are given in Table 4.

Figure 15 presents the RDR variation with geocell height, h/D for number of load cycles. It can be seen that the percentage reduction in rut depth is as high as 90 % for the first few loading cycles and gradually reduced to 75 %. The reduction in rut depth increased with increase in h/D until 0.67 . Further increase in height of geocell beyond $h/D = 0.67$ has no influence on the RDR.

Hence, the geocell of size $h/D = 0.67$ and $b/D = 4.33$ has been providing highest resilient behavior during the repeated traffic loading in this study. This is considered as the optimum height of the geocell mattress for sand subgrades based on RDR.

Influence of Geocell Seam Strength

The performance of commercially available geocells is dependent on the seam strength of geocells. To visualize the influence of geocell seam strength on overall

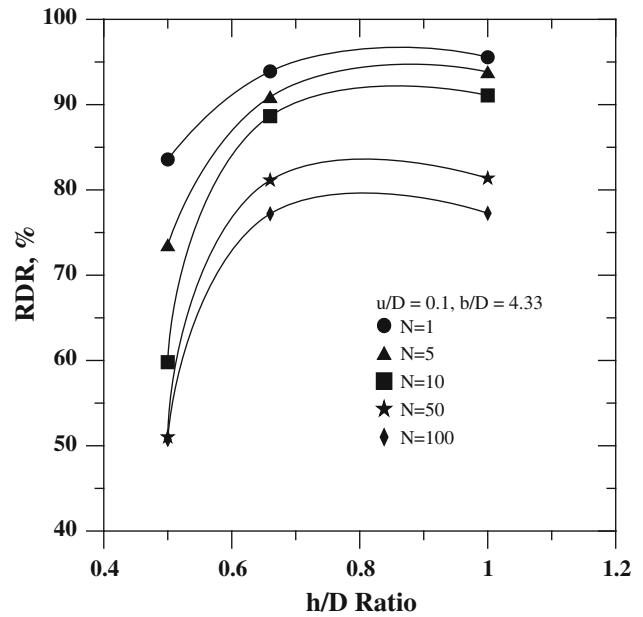


Fig. 15 Variation of RDR with h/D ratio—Series C

performance of geocell reinforced sand subgrades, test series-D was carried on single geocell with a loading on seam directly and loading on geocell pocket. In these tests, geocell of size $h/D = 1.0$ and $b/D = 2.33$ were considered to maintain the same amount of reinforcement available in both the cases. The influence of geocell seam strength is assessed based on the CPDs, TBRs and visual inspection of post-test exhumed geocell materials.

The variation of CPDs with number of loading cycles is shown in Fig. 16. The variation of TBR with settlement ratios for this series is presented in Fig. 17. It is noticed that the CPDs are higher in the case of load application on geocell pocket than on the seam/weld. This reduction in CPDs (i.e. RDR) in the case of seam and cell pocket is about 2 and 1.5 fold respectively against unreinforced subgrade. This indicates that the loading on seam provides higher resistance to rutting before it fails. However, post-test exhumed geocell samples have shown that the seams were ruptured due to repeated traffic loading. Both the configurations of geocells behaved same in terms of TBRs at $s/D = 10$ %. The TBRs at 10 % settlement ratio are observed to be 2 for both cell and seam, however, for higher settlement ratios ($s/D > 10$ %), seam performed better than the load on geocell pocket.

Table 4 summarizes the results from test series A–C. It can be compared that the CPDs have come down from 72 to 13 % as size of the geocell mattress increased to its optimum size. Similarly, the modulus of subgrade reaction and resilient modulus have increased with increase in the geocell geometry. From the data presented in Table 4, it can be inferred that the performance of the geocell reinforced sand

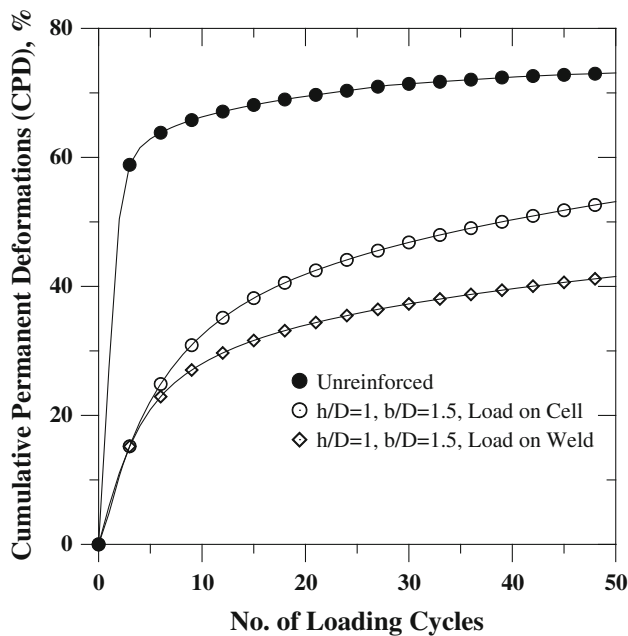


Fig. 16 Variation of CPD with number of cycles—Series D

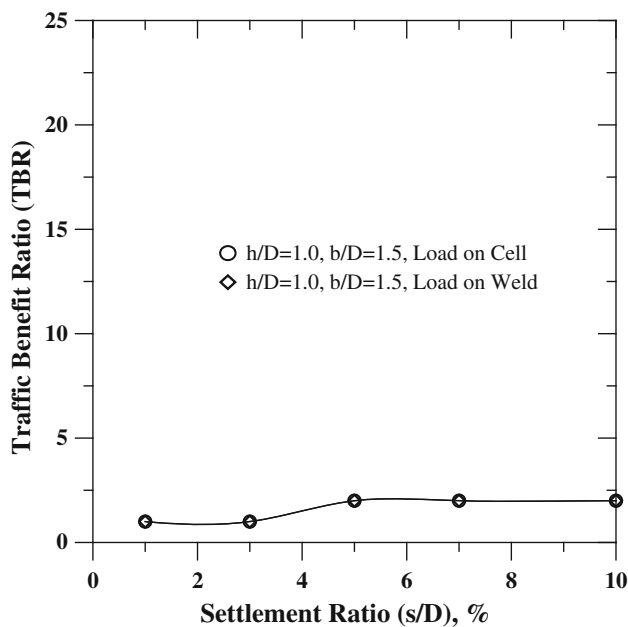


Fig. 17 Variation of TBR with settlement ratio—Series D

subgrades have increased when the size of the geocell reaches its optimum ($b/D = 4.33$ and $h/D = 0.67$).

Conclusions

- 1 Geocell can be effectively used as a reinforcement system in pavement subgrades to increase the stiffness and resilient behavior of the subgrades.

- 2 A reduction in cumulative permanent deformations, CPDs are observed for increase in the geometry of the geocell in terms of width and height. A 4 fold reduction in cumulative permanent deformations were observed for a geocell geometry of $b/D = 4.33$ and $h/D = 0.67$. Similar reductions in CPDs are observed even if the height of the geocell was increased from 0.67 to 1. The first case being encapsulating all the potential failure surfaces within the geometry of the geocell, further increase in height of geocell did not show any improvement in terms of CPDs.
- 3 Traffic benefit ratio calculated at 10 % of loading plate settlement has increased with increase in the geometry of the geocell. A TBR of as high as 23 was observed for $h/D = 1.0$ and $b/D = 4.33$.
- 4 It was noticed that the seam strength of geocell mattress has a critical influence on the overall performance of the geocell reinforced sand subgrades. The geocell seam has provided higher structural support to the loading system than the case of load application on geocell pockets.
- 5 The percentage reduction in rut depth, RDR, increased with increase in h/D until 0.67. Further increase in height of geocell beyond $h/D = 0.67$ has no influence on the RDR. Hence, the geocell of size $h/d = 0.67$ and $b/d = 4.33$ providing highest resilient behavior during the repeated traffic loading is considered as optimum size of geocell mattress for sand subgrades in this study.
- 6 The maximum value of $k_s = 588 \text{ MN/m}^3$ and $M_r = 88 \text{ MPa}$ was observed in case of $h/D = 1.0$ and $b/D = 4.33$.
- 7 Overall, it can be summarized that the geocell of sufficient height (h) and width (b) will provide a higher TBR and least rut depth for a given level of traffic loading conditions. For the present study, a geocell geometry of $b/D = 4.33$ and $h/D = 0.67$ performs better in terms of rutting characteristics of subgrades.

Acknowledgments The authors would like to express their sincere appreciation to Department of Science and Technology (DST) for providing research funding to carry out this study. Authors also acknowledge STRATA Geosystems India Pvt. Ltd. for providing the geocell material for this research.

References

1. Webster SL (1979) Investigation of beach and trafficability enhancement using sand-grid confinement and membrane reinforcement concepts. Report GL-79-20, US Army Engineer Waterways Expt Station, Vicksburg, MS, USA

2. Giroud JP, Noiray L (1981) Geotextile reinforced unpaved road design. *Geotech Eng Div J* 107:1233–1254
3. Dash SK, Krishnaswamy NR, Rajagopal K (2001) Bearing capacity of strip footings supported on geocell-reinforced sand. *Geotext Geomembr* 19(4):235–256
4. Han J, Yang XM, Leshchinsky D, Parsons RL (2008) Behavior of geocell-reinforced sand under a vertical load. *Transp Res Board J* 2045:95–101
5. Zhou H, Wen X (2008) Model studies on geogrid or geocell-reinforced sand cushion on soft soil. *Geotext Geomembr* 26(3):231–238
6. Barksdale RD, Brown SF, Chan F (1989) Potential Benefits of geosynthetics in flexible pavement systems, NCHRP Report No. 315, Transportation Research Board, Washington, DC, USA
7. Cancelli A, Montanelli F (1999) In-ground test for geosynthetic reinforced flexible paved roads. In: *Proceedings of the geosynthetics international conference*, Boston, MA, USA, vol 2, pp 863–878
8. Collin JG, Kinney TC, Fu X (1996) Full scale highway load test of flexible pavement systems with geogrid reinforced base courses. In: *Proceedings of the geosynthetics international conference*, Roseville, MN, vol 3, pp 537–549
9. Dash SK, Sireesh S, Sitharam TG (2003) Model studies on circular footing supported on geocell reinforced sand underlain by soft clay. *Geotext Geomembr* 21(4):197–219
10. Sitharam TG, Sireesh S (2005) Behaviour of embedded footings supported on geocell reinforced foundation beds. *ASTM Geotech Test J* 28:452–463
11. Bender DA, Barenberg EJ (1980) Design and behavior of soil-fabric-aggregate systems. *Transp Res Record J TRB* 671:64–75
12. Kinney TC, Barenberg EJ (1982) The strengthening effect of geotextiles on soil-geotextile-aggregate systems. In: *Proceedings of the second international conference on geotextiles*, Las Vegas, NV, USA, vol 2, pp 347–352
13. Hossein M, Kazemian S, Arun P, Bujang BK, Huat (2009) Effect of geogrid reinforcement location in paved road improvement. *Electron J Geotech Eng* 14:1–11
14. Barker WR (1987) Open-graded bases for airfield pavements, Technical Report GL-87-16, USAE Waterways Expt Station, Vicksburg, MS, USA
15. Haas R, Wall J, Carroll RG (1988) Geogrid reinforcement of granular bases in flexible pavements. *Transp Res Rec J TRB* 1188:19–27
16. Al-Qadi IL, Brandon TL, Valentine RJ, Lacina BA, Smith TE (1994) Laboratory evaluation of geosynthetic reinforced pavement sections. *Transp Res Rec J TRB* 1439:25–31
17. Pokharel SK (2010) Experimental study on Geocell-reinforced bases under static and dynamic loading. D Phil Thesis, University of Kansas, USA
18. Saride S, Vijay KR, Suraj V, Anand JP (2013) Repeated load tests on geocell reinforced sand subgrades. In: *Proceedings of the geosynthetics international conference*, Long Beach, CA, vol 3, No. 4, pp 537–549
19. Kazerani B, Jamnejad G (1987) Polymer grid cell reinforcement in construction of pavement structures. Section 1A, unpaved and paved roads. In: *Proceedings of the geosynthetics international conference*, New Orleans, USA
20. ASTM Standard D422 (2007) Standard test method for particle size analysis of soils, ASTM International, West Conshohocken, PA. www.astm.org
21. ASTM D 854 (2000) Standard test for specific gravity of soil solids by water pycnometer. ASTM International, West Conshohocken, PA. www.astm.org
22. ASTM D 4253 (2006) Standard test methods for maximum index density and unit weight of soils using a vibratory Table, ASTM International, West Conshohocken, PA. www.astm.org
23. ASTM D 4254 (2006) Standard test methods for minimum index density and unit weight of soils and calculation of relative density. ASTM International, West Conshohocken, PA. www.astm.org
24. ASTM D 3080 (1998) Standard test method for direct shear test of soils under consolidated drained conditions. ASTM International, West Conshohocken, PA. www.astm.org
25. Chummar AV (1972) Bearing capacity theory from experimental results. *J Geotech Eng ASCE* 98(12):1311–1324
26. Edil TB, Fratta D, Shuettpelz CC (2009) development of testing methods to determine interaction of geogrid-reinforced granular material for mechanistic pavement analysis. Wisconsin DOT and FHWA Project Report
27. Saride S, Gautam D, Madhav MR, Vijay KR (2014) Performance evaluation of geocell reinforced granular subbase (GSB) layers through field trials. *J Indian Roads Congr*, No. IRC-6(5)/2014 (under review)
28. Moghaddas Tafreshi SN, Dawson AR (2012) A comparison of static and cyclic loading responses of foundations on geocell-reinforced sand. *Geotext Geomembr* 32:55–68
29. Shin EC, Das BM, Lee ES, Atalar C (2002) Bearing capacity of strip foundation on geogrid-reinforced sand. *Geotech Geol Eng* 20:169–180
30. Fabymole PA, Sireesh S, Madhav MR (2014) Numerical modelling of strip footing on geocell-reinforced beds. In: *Proceedings of the institution of civil engineers ground improvement*, vol 167. doi:10.1680/grim.13.00015